Flexural vibrations induced in thin metal wires carrying high currents

To cite this article: A Lukyanov and S Molokov 2001 *J. Phys. D: Appl. Phys.* **34** 1543

View the article online for updates and enhancements.

Related content

Recent citations

IOP ebooks™

Bringing you innovative digital publishing with leading voices to create your essential collection of books in STEM research.

Start exploring the collection - download the first chapter of every title for free.

Flexural vibrations induced in thin metal wires carrying high currents

A Lukyanov and S Molokov

School of Mathematical and Information Sciences, Coventry University, Priory Street,
Coventry CV1 5FB, UK

Abstract
Exploding wires are widely used in many experimental set-ups and pulsed
power systems such as Z-pinch, high-current switches, copper-vapour lasers
and high-brightness x-ray lithography. However, many aspects of the
process of wire explosion still remain unclear. If the current density is not
too high, the wire may break up in the solid state. The experiments have
shown that the wires break in tension due to longitudinal forces of unknown
nature. Previous theoretical and numerical investigations served to provide a
search for these forces and have identified the pinch effect and thermal
expansion as a source of strong longitudinal vibrations. But the mechanism
does not give a satisfactory explanation for the phenomenon in the wires
with clamped ends. In this investigation, we use a simplified
magneto-thermo-elastic model to study flexural vibrations induced by high
pulsed currents in wires with clamped ends on account of their role in the
disintegration process. Several aspects are studied, namely (i) the buckling
instability due to simultaneous action of the thermal expansion and the
magnetic force, and (ii) the flexural vibrations induced in initially bent
wires. It is shown that the induced flexural vibrations are strong enough to
lead to the breaking of the wire in a wide range of parameters.

1. Introduction

The phenomenon of wire fragmentation in the solid state
by high pulsed currents was studied experimentally by
Nasilovski [1], and Graneau [2–4]. They observed that a
sufficiently strong electric current would shatter a thin metal
wire under a broad range of conditions (various wire material
and geometry, different current types, etc). As a result of
the explosion the wires fragmented into 2–100 pieces with
apparent signs of longitudinal tensile stress. The experimental
results, as well as (sometimes controversial) early attempts to
explain the phenomenon, have been reviewed by Graneau [5],
Hong [6] and Molokov and Allen [7].

It is obvious that an electric current passing through a
metal wire induces stress waves. Their origins are in (i) the
thermal expansion owing to the volumetric joule heating, and
(ii) the Lorentz force.

Ternan [8] suggested that in Graneau's experiments with
wires with free ends, standing stress waves may be induced as
a result of thermal expansion. Using a simple one-dimensional
model he showed that the resulting stresses were sufficient to
lead to a fracture.

This mechanism of fragmentation of wires with free ends
has been explored in more detail by Molokov and Allen

in [7]. They employed a magneto-thermo-elastic model of the
stress-wave propagation, and solved the problem numerically
on the assumption of the axisymmetric nature of vibrations.
Their conclusion was that the characteristic value of both
compressive and tensile longitudinal stresses obtained for the
aluminium wire with radius $a = 0.6$ mm carrying current
$I = 5$ kA and having free ends (the parameters relevant to the
experiment in [3]) would be about 33 MPa per unit length of the
wire. The stress has been shown to grow linearly with the wire
length and thus, for sufficiently long wires, the resultant stress
exceeds the ultimate strength of aluminium. This is 75 MPa at
$100\,°C$ going down to 17 MPa at $320\,°C$ [9].

Although the mechanism does give large values of tensile
stresses, it cannot explain the fragmentation of wires with
clamped ends (as in the experiments [1, 4]) because within
the axisymmetric model in this case the stresses can be only
compressive [7]. It is clear, however, that in the wires with
clamped ends flexural vibrations may be induced. Apparent
signs of these modes have been observed in Graneau's
experiments [4] on the wires with firmly clamped ends.

In this paper we carry out a special study of flexural
vibrations to account for their role in the fragmentation of wires
with clamped ends. In section 2 we present the formulation

of the problem and discuss simplifications of the model. In section 3 the linear stability of the system is considered. In section 4 we carry out a qualitative analysis of expected stresses. In section 5 a numerical algorithm and results are presented.

2. Formulation

Consider a wire which is firmly clamped between two points located along the z-axis. Let the distance between these points be L. We restrict our attention to the case of plane motion, and denote the deflection of the wire from the axis by X which is a function of z and time t. The deflection of the wire in the initial undeformed state is denoted by X_0. Possible three-dimensional modes, not considered here, may only increase stresses, especially at the clamped ends.

Our theoretical consideration is based on a simplified model valid for sufficiently long or sufficiently thin wires. In this model the deflection X of the wire is assumed to be much lower than the wire length, i.e. $|X|/L \ll 1$. Since large deflections of the order of the wire length are not expected in the wire explosion experiments, this restriction is not expected to be very stringent. Another small parameter used in the model is the ratio $a/L \ll 1$, where a is the wire radius. This condition is usually well satisfied. Plastic deformations are not considered here, although they may be important in the vicinity of the melting point. Thus all deformations are assumed to be elastic.

Then the deflection X obeys the following equation [10]:

$$\rho S \frac{\partial^2 X}{\partial t^2} + EJ \frac{\partial^4 X}{\partial z^4} - EJ \frac{\partial^4 X_0}{\partial z^4} - G \frac{\partial^2 X}{\partial z^2} - F_x - \frac{\partial C_y}{\partial z} = 0 \quad (1)$$

where ρ is the material density, S is the wire cross section which may be a function of z, J is the effective moment of inertia of the wire cross section (for a circular cross section $J = \pi a^4/4$, where a is the wire radius), E is Young's modulus, G is the force along the z-axis applied at the wire ends, F_x is the distributed external force per unit length along the x direction and C_y is the distributed moment of force along the y direction per unit length.

For the physical situation considered here, the force G can be represented as

$$G = ES\{(\tilde{l} - \tilde{l}_0)/L - \alpha[T(t) - T_0]\}. \quad (2)$$

The second term is a compressive force due to the thermal expansion, α being the linear expansion coefficient. The first, nonlinear term is a retarding force due to the wire deformation from the initial state, where

$$\tilde{l} - \tilde{l}_0 = \frac{1}{2} \int_0^L \left(\frac{\partial X}{\partial z}\right)^2 - \left(\frac{\partial X_0}{\partial z}\right)^2 \mathrm{d}z \quad (3)$$

is the increment of the wire length due to the deflection. When $X = X_0$, $\tilde{l} = \tilde{l}_0$ and the retarding force equals zero, as required.

The boundary conditions are those for the clamped ends, namely

$$X = \frac{\partial X}{\partial z} = 0 \qquad \text{at } z = 0 \text{ and } z = L. \quad (4)$$

The initial conditions are

$$X = X_0, \qquad t = 0. \quad (5)$$

2.1. The magnetic force

In long, thin wires under consideration $a/L \ll 1$, the uniform current is directed perpendicular to the cross section. Thus any possible forces of a magnetic nature act only in the cross sectional plane. These forces create no moment and thus $C_y = 0$ in our case.

The net distributed force $\boldsymbol{F}$ can be calculated directly from

$$\boldsymbol{F} = \int \boldsymbol{j} \times \boldsymbol{B} \, \mathrm{d}S. \quad (6)$$

The integral in (6) is taken over the wire cross section area. The magnetic field is given by the Biot–Savart law

$$\boldsymbol{B} = \frac{\mu_0}{4\pi} \int \frac{\boldsymbol{j} \times \boldsymbol{R}}{R^3} \mathrm{d}V' \quad (7)$$

where $\mathrm{d}V'$ is the volume element on the wire, $\boldsymbol{j}$ is the current density, and the vector $\boldsymbol{R} = \boldsymbol{r} - \boldsymbol{r}'$ is directed to the field point as usual.

To calculate the x component of the force, F_x, one can split the integral (7) over the wire length z' into two parts $\boldsymbol{B} = \boldsymbol{B}_{in} + \boldsymbol{B}_{ex}$. The first part of the integral $\boldsymbol{B}_{in}$ is taken over the range $|z' - z| < \Delta$, where $a \ll \Delta \ll \xi_L$, ξ_L being the characteristic length scale of the function $X(z)$. The second part $\boldsymbol{B}_{ex}$ is taken over the rest of the wire length $\Delta < |z' - z| < L$, whereby the volume integral reduces to the integration over the wire length only. That is,

$$\boldsymbol{B}_{ex} = \frac{\mu_0}{4\pi} \int \frac{\boldsymbol{I} \times \boldsymbol{R}}{R^3} \mathrm{d}l'$$

where I is the total current. The first integral can be evaluated in general with the assumption of a uniform current distribution and in the approximation $a \ll \xi_L$, $|X|/\xi_L \ll 1$. The first inequality has been implicitly introduced in fact when we set the length Δ; the second inequality just represents the fact that the wire is slightly deflected from a straight line. The first integration asymptotically gives the expression for the net force as follows

$$\{F_x\}_{in} = -\frac{\mu_0 I^2}{4\pi} \frac{\partial^2 X}{\partial z^2} \{\ln(2\Delta/a) - 3/4\}$$
$$+ O((X/\xi_L)^2, \Delta/\xi_L, (a/\Delta)^2). \quad (8)$$

That is the force is proportional to the local wire curvature [11]. The second part cannot be integrated in a general case and one needs to make certain assumptions about the wire form and thus about the function $X(z)$ itself. In the case of an infinitely long wire with periodic lateral perturbations $X = \tilde{X}\cos(kz)$, $k = 2\pi/\xi_L$, one gets

$$\{F_x\}_{ex} = -\frac{\mu_0 I^2}{4\pi} \frac{\partial^2 X}{\partial z^2} \{-C + 1/2 - \ln(k\Delta)\}$$
$$+ O(k\Delta, (X/\xi_L)^2, (a/\Delta)^2) \quad (9)$$

where $C = -\int_0^\infty e^{-t} \ln t \, \mathrm{d}t \simeq 0.577$ is Euler's constant and we have substituted $Xk^2 = -\partial^2 X/\partial z^2$. Combining two parts we obtain

$$F_x = -\frac{\mu_0 I^2}{4\pi} \frac{\partial^2 X}{\partial z^2} \{\ln(2/ka) - C - 1/4\}. \quad (10)$$

Note, that the expression (10) is identical to the formula obtained in [12] in a particular case of small periodic deflections $|X| \ll a$.

It is clear that the assumption of an infinitely long wire to calculate the force, F_x, is not very rigorous, since in experiments the circuit is always closed. This implies that in addition to the magnetic force by the wire current itself, there may be a component generated by the currents flowing in the external circuit. This effect can be taken into consideration by substituting an appropriate circuit form, in other words the function $X(z)$ in the second integral.

Alternatively, this force can be obtained by means of the virtual work principle. To estimate how strong the effect could be, we will use a general expression for the inductance of a closed circuit $\Lambda = (\mu_0/2\pi)L_s \ln(L_s/a_s)$, where L_s is the circuit characteristic length and a_s is the radius of the circuit wire, see [13]. Then by varying the circuit length L_s one can calculate the subsequent variation of the associated magnetic energy $E_m = \frac{1}{2}\Lambda I^2$. Equalizing the net force acting on the circuit F_N with the variation of the energy we get

$$F_N \delta L_s = \frac{\mu_0}{4\pi} I^2 (\ln(L_s/a_s) + 1)\delta L_s. \tag{11}$$

An average force acting on a unit length is $f = F_N/L_s$. Then, for the average force from (11) we get

$$f \simeq \frac{\mu_0}{4\pi} I^2 (\ln(L_s/a_s) + 1)/L_s. \tag{12}$$

The first, logarithmic part of the net force represents contributions from the end effects, see (8). The second part gives the integrated force from the circuit as a whole. If $L \ll L_s$, one can assume that the force is constant throughout the wire length in the first approximation. Then, this 'constant' force acting on a wire of length L will bend it and create longitudinal stress. The form of the bent wire and the magnitude of the longitudinal stress $\sigma_\parallel = G/S$ can be found from equation (1), which in this case assumes a form

$$EJ\frac{\partial^4 X}{\partial z^4} - G\frac{\partial^2 X}{\partial z^2} = f \tag{13}$$

with the boundary conditions (4). In the case $X < a$, one can neglect the second term in (13). The particular solution of (13) satisfying (4) has then the form

$$X = \frac{fz^2(z-L)^2}{24EJ}. \tag{14}$$

Neglecting the thermal expansion term in (2) and substituting (14), for the longitudinal stress one gets

$$\sigma_\parallel = \frac{L^6 f^2}{60\,480\,EJ^2}. \tag{15}$$

In another limit case, when $X \gg a$, the particular solution of (13) satisfying (4) is

$$X = \frac{f(L-z)z}{2G}. \tag{16}$$

Then, substituting (16) into (2), for the longitudinal stress one gets

$$\sigma_\parallel = \left(\frac{f^2 EL^2}{24S^2}\right)^{1/3}. \tag{17}$$

Substituting f from (12) into (15) and (17) one can obtain

$$\sigma_\parallel = \frac{\mu_0^2 I^4}{60\,480} \frac{\ln(L_s/a_s)^2}{E(\pi a^2)^4} \frac{L^6}{L_s^2} \tag{18}$$

in the first case and

$$\sigma_\parallel = \left(\frac{\mu_0^2 I^4 \ln(L_s/a_s)^2 EL^2}{384\pi^2 L_s^2 S^2}\right)^{1/3} \tag{19}$$

in the second case. For a copper wire with $L = 30$ cm, $a = 0.6$ mm and the circuit with $I = 5$ kA, $L_s = 20$ m and $a_s = 1$ cm, the characteristic maximal deflection is $X \simeq 2a$. Thus, the case is contained between two asymptotics for these particular values of parameters. The stress amounts to $\sigma_\parallel \simeq 8.4$ MPa being calculated by means of (18) and $\sigma_\parallel \simeq 6.9$ MPa being calculated by means of (19). It is seen that both formulae gave approximately the same answers. Obviously, while $X \simeq 2a$, the actual magnitude of the longitudinal stress must be close to those asymptotic values. This is only an estimation, and the effect needs special analysis since the geometry of external circuits is usually unknown. For example, using a symmetrical circuit with two loops from both sides of the wire one can completely compensate for the external magnetic force.

We leave this question for further detailed investigation and neglect the contribution from the external circuit in our analysis. Further we will use formula (10).

2.2. The temperature behaviour

The temperature behaviour with time is governed by the passing current. It can be calculated according to the direct joule heating of the wire material from

$$\rho c_v \frac{\partial T}{\partial t} = j^2/\sigma \tag{20}$$

neglecting the process of thermal conductivity. This assumption would hold for thermally isolated wires with uniform current distribution. In expression (20), j is the current density, ρ and σ are the density and the electrical conductivity of the metal, c_v is the specific heat. From the above equation using the well known inverse dependence of the conductivity on temperature, $\sigma = \sigma_0 T_0/T$, one can obtain

$$T = T_0 \exp\left(\gamma_T \int_0^t f(t')^2 \, dt'\right)$$

where $\gamma_T = j_0^2/\sigma_0 T_0 \rho c_v$ is the characteristic temperature rise time, j_0 is maximum current density. The function $f(t)$ defines the current rise time profile.

3. Linear stability

To investigate possible instabilities in the system, we first carry out a linear stability analysis assuming for a moment that all the parameters, such as current and wire temperature, are constants independent of time. Even though, in a real situation, they vary quite fast with time and numerical methods must be involved to solve the system, our simplified analysis will form a basis for qualitative interpretation and understanding of the results.

3.1. Stability of an initially straight wire

Consider an initially straight wire by letting $X_0 = 0$. General analysis of the system (1) shows that two basic types of buckling instabilities may develop. They are due to thermal expansion, expressed by the force G applied at the wire ends [10], and the magneto-elastic buckling instability [14] expressed by force F_x. In both cases, the instability has a threshold character. When either the force G or the current I exceed some critical value, new stable states appear. The initially stable state $X = 0$ then becomes unstable and buckling occurs.

We are looking for non-trivial stationary solutions of the linearized system (1), (4), (5). They are given by the equation

$$EJX^{IV} - GX'' - F_x = 0 \qquad (21)$$

with the boundary conditions

$$X = X' = 0 \qquad \text{at } z = 0 \text{ and } z = L. \qquad (22)$$

Here, the temperature, T, and the total current, I, are assumed to be independent of time, and so are the functions G and F_x given by (2) and (10), respectively. Further, G is linearized to give $G = -\alpha ES[T - T_0]$.

To obtain a solution to (21) it is convenient to use a complete set of orthogonal functions $\{\mathcal{X}_i\}$, $i \geqslant 1$ defined by the problem

$$\mathcal{X}_i^{IV} + \lambda_i^2 \mathcal{X}_i'' = 0$$
$$\mathcal{X}_i'(0) = \mathcal{X}_i'(L) = \mathcal{X}_i(0) = \mathcal{X}_i(L) = 0 \qquad (23)$$

with the orthogonality given by

$$\int_0^L \mathcal{X}_i'' \mathcal{X}_k'' \, \mathrm{d}z = \begin{cases} 0 & i \neq k \\ \dfrac{\lambda_i^4}{2} L & i = k \end{cases}$$

$$\int_0^L \mathcal{X}_i' \mathcal{X}_k' \, \mathrm{d}z = \begin{cases} 0 & i \neq k \\ \dfrac{\lambda_i^2}{2} L & i = k. \end{cases} \qquad (24)$$

This set of functions is commonly used in the theory of stability and buckling of elastic columns [15].

The eigenvalues of the boundary-value problem (23) satisfy the dispersion equation

$$1 - \cos(\lambda_i L) = \frac{\lambda_i L}{2} \sin(\lambda_i L) \qquad (25)$$

so, one can see that the set of functions consists of two subsets. The first subset is defined by the eigenvalues given by

$$\cos(\lambda_i L) = 1 \qquad \sin(\lambda_i L) = 0. \qquad (26)$$

that is

$$\lambda_i = \pi(i+1)/L \qquad i = 1, 3, 5 \ldots.$$

In this case the associated eigenfunctions are given by

$$\mathcal{X}_i = \cos(\lambda_i z) - 1. \qquad (27)$$

The second subset is defined by

$$\cos(\lambda_i L) = \frac{4 - (\lambda_i L)^2}{4 + (\lambda_i L)^2} \qquad \sin(\lambda_i L) = \frac{4\lambda_i L}{4 + (\lambda_i L)^2}. \qquad (28)$$

The associated eigenfunctions are given by

$$\mathcal{X}_i = \cos(\lambda_i z) - 1 + 2z - \frac{2}{\lambda_i L} \sin(\lambda_i z). \qquad (29)$$

The first eigenvalue of this subset is equal to $\lambda_2 = 8.986\,819/L$. Further eigenvalues are approximately given by $\lambda_i \simeq \pi(i+1)/L$, $i = 4, 6, 8 \ldots$.

Now, with the help of (24) one can obtain from (21) a criterion when the instability first appears

$$\alpha(T - T_0)ES - \frac{\mu_0}{4\pi} I^2 (\ln(\lambda_1 a) + 0.14) > EJ\lambda_1^2. \qquad (30)$$

The first term on the left-hand side of (30) is responsible for the thermal expansion effect, while the second term represents magneto-elastic buckling. It should be noted that while we are considering both effects simultaneously, for parameters relevant to wire explosion experiments these terms have different orders of magnitude.

The criterion obtained shows when the first eigenmode of (1) and the system as a whole become unstable, $\lambda_1 = 2\pi/L$ being the corresponding eigenvalue. In a similar manner, substituting other eigenvalues λ_i for λ_1, one can obtain respective criteria for higher modes as well.

The set (23) being very useful in the linear stability analysis of system (1) does not seem to be very relevant to a study of the increments of the instability since

$$\int_0^L \mathcal{X}_i \mathcal{X}_k \, \mathrm{d}z \neq 0 \qquad i \neq k.$$

However, it would be interesting to obtain an estimate of the increments of the instability. For this purpose, we will substitute a solution to (1) in the form of $X = A_i(t)X_i$, i.e. assuming that only one mode is present. Then, for the increment γ_i, $(A_i(t) \sim \exp(\gamma_i t))$, one gets

$$\gamma_i^2 = \frac{E}{\rho} \frac{\lambda_i^2}{2} \frac{L}{\int_0^L X_i^2 \, \mathrm{d}z} \left\{ \Xi - \lambda_i^2 \frac{J}{S} \right\}$$

$$\Xi = \alpha(T - T_0) - \frac{\mu_0 I^2}{4\pi ES} \{0.14 + \ln(a\lambda_i)\} \qquad (31)$$

or since $\int_0^L X_i^2 \, \mathrm{d}z \simeq L$

$$\gamma_i \simeq \sqrt{\frac{E}{\rho}} \lambda_i \left\{ \Xi - \lambda_i^2 \frac{J}{S} \right\}^{1/2}. \qquad (32)$$

As is seen from (32), the increment has a maximum at $\lambda_i = \lambda_{ext}$ defined by the equation

$$\lambda_{ext}^2 = \frac{S}{J} \frac{\alpha(T - T_0)}{2} - \frac{\mu_0 I^2}{8\pi EJ} \{0.64 + \ln(a\lambda_{ext})\}. \qquad (33)$$

As we will see further, for the range of parameters used in the wire explosion experiments, the contribution from the terms due to magnetic force can be neglected during the initial stage and within this approximation, using explicitly $J = \pi a^4/4$ and $S = \pi a^2$,

$$\lambda_{ext} = \sqrt{\frac{2\alpha(T - T_0)}{a^2}}. \qquad (34)$$

Table 1. Parameters for wire fragmentation experiments.

	Material	a (mm)	L (m)	I	P_1	P_2	P_3
A	Aluminium	0.6	0.05	5 kA	1.19×10^3	6.11	114
B	Aluminium	0.6	1	5 kA	1.19×10^3	13.6	0.28
C	Aluminium	0.6	1	2 kA	1.19×10^3	2.18	0.28
D	Aluminium	0.6	1	8 kA	1.19×10^3	34.8	0.28
E	Copper	0.5	1	500 A	1.84×10^3	0.14	0.24

Since $\lambda_i \simeq \pi(i + 1)/L$,

$$i_{ext} = \sqrt{\frac{2\alpha(T - T_0)}{a^2} \frac{L}{\pi} - 1}. \qquad (35)$$

On the other hand, the maximal λ_{lim} at which instability may exist is obtained from (32) to give

$$\lambda_{lim} \simeq 2\sqrt{\frac{\alpha(T - T_0)}{a^2}} \qquad (36)$$

with the same accuracy. From (36), since $\lambda_i \simeq \pi(i + 1)/L$, one gets for the maximal mode number

$$i_{lim} \simeq 2\sqrt{\frac{\alpha(T - T_0)}{a^2}} \frac{L}{\pi} - 1. \qquad (37)$$

Thus the dominant mode lies somewhere between the first and the last unstable mode with the maximal increment

$$\gamma_{ext} = \sqrt{\frac{E}{\rho} \frac{\alpha(T - T_0)}{a}}. \qquad (38)$$

From expression (35) one can see that higher modes are likely to become dominant in the instability spectrum with increases in the wire length. As a result, the wire shape can take a rather intricate form. It seems that the instability of higher modes has been observed experimentally by Graneau [4]. For the experimental conditions he used, i.e. aluminium wire, $L = 1$ m, $a = 0.6$ mm, from (34) one gets $\lambda_{ext} \simeq 294$ or the corresponding mode number $i_{ext} = 93$ at $T = T_{melt}$. The photographs of the wire shape after the current had been switched off clearly showed the appearance of at least five bulges on a small part of the wire.

We will refer further to the sets of parameters presented in table 1 corresponding to different wire lengths and different currents. One should note that two sets, [B] and [E], are relevant for wires and currents used in experiments [1, 4], respectively. For all the represented sets, criterion (30) is fulfilled well enough. Indeed, we have put in table 1 the corresponding values of the terms in (30), designating them as P_1, P_2 and P_3 from left to right. The estimations have been done at $T = T_{melt}$, T_{melt} being the melting temperature; $T_{melt} = 660\,°$C for aluminium and $T_{melt} = 1085\,°$C for copper. The characteristic increment (38) at the same conditions, in case [B] for instance, is $\gamma_{max} \simeq 10^5$ s^{-1}, which is much greater than the temperature increment $\gamma_T \simeq 7 \times 10^2$ s^{-1}. Thus, even though the estimation has been done in the linear approximation, it is clear that the instability has sufficient time to develop before the wire reaches the melting point.

In all the cases, as is seen, the major contribution is from the thermal expansion effect, while the influence of the magnetic force terms can be neglected during the initial stage (this, of course, can be estimated directly from (1) as well). Two terms, P_1 and P_2, for instance in case [B], become equal only at $T - T_0 = 6.6\,°$C. The time it takes for the temperature to be driven through this range is $\Delta t \simeq 30$ μs. The characteristic time for the instability to develop for this temperature difference is much longer, $\gamma_{max}^{-1} = 800$ μs.

3.2. Stability of an initially bent wire

Consider a wire which has an initial form $X_0 = \sum_i A_i^0 \mathcal{X}_i$, where the functions $\{\mathcal{X}_i\}$ are the set (23) and A_i^0 are given weight coefficients. One needs to stress that with the accuracy to which the system (1) was derived, $|X_0| > a$ must always be the case. Performing an analysis similar to that leading to equation (30) and neglecting the magnetic force for the sake of simplicity, for a mode k one gets

$$\lambda_k^2(A_k - A_k^0)EJ - A_k ES(\alpha\Delta T) = 0. \qquad (39)$$

From (39) one can see that there is always a stationary state which differs from X_0 at any nonzero value of the parameter $\alpha\Delta T$. Thus, those modes which have $A_k^0 \neq 0$ are always unstable. The result is not surprising, since from the physical point of view it is obvious that a constantly heated wire will change its form owing to expansion. On the other hand, those modes which have $A_k^0 = 0$ become unstable at some value of the parameter $\alpha\Delta T$, so that buckling instability is still possible on these modes.

4. Qualitative stress analysis

Once the instability occurs, all the potential energy within the compressed wire can be quickly released. The characteristic value of the longitudinal stress τ_{zz} which may be accumulated during the preconditioning is within the interval between the maximum value $\tau_{zz}^{max} = \alpha(T_{melt} - T_0)E \sim 10^3$ MPa and the minimum value $\tau_{zz}^{min} = E(J/S)\lambda_0^2 \simeq 0.3$–30 MPa, corresponding to the onset of the instability. The estimation has been done for an aluminium wire of radius $a = 0.6$ mm and the length spanning the range 1 m $> L > 0.05$ m.

One can see, that the maximum value itself is very high, about ten times higher than the ultimate strength value. On the other hand, the minimum value can be quite small, depending on the wire length. The average transverse stress is given by

$$\langle \tau_{xx} \rangle = \frac{G}{S}X' - E\frac{J}{S}X'''. $$

For small deflections, $|X|/\xi_L \ll 1$, it is in general smaller then the longitudinal value.

From the qualitative point of view it is evident that the maximal stress energy can be accumulated if the temperature
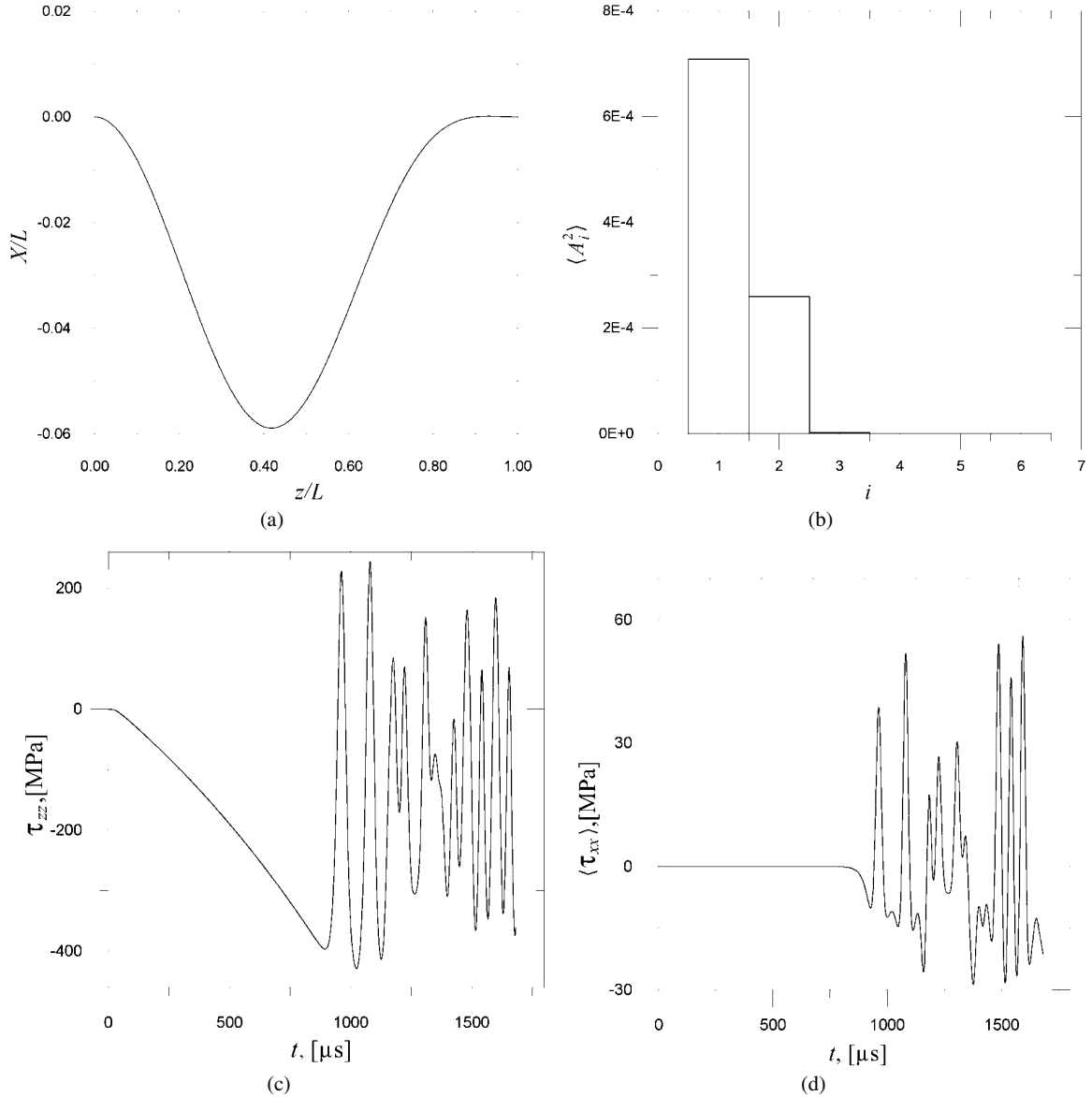
Figure 1. (a) The wire displacement X/L as a function of z/L, case [A]. (b) The spectrum of the wire vibrations at the melting point $\langle A_i^2 \rangle$ as a function of mode number i, case [A]. (c) The longitudinal stress τ_{zz} as a function of time, case [A]. (d) The transverse stress $\langle \tau_{xx} \rangle$ as a function of time at $z/L = 0.9$, case [A].

rises sufficiently quickly. The temperature rise time must be shorter or comparable with the rise time of the instability. The most dramatic result might be expected if the wire is heated up to the temperature just slightly below the melting point. Then the current is switched off thus allowing the instability to develop without melting the material. On the other hand, if the current is low and, as a consequence, the temperature rise time is low too, then all the accumulated energy can be released at the onset of the instability by the first mode which becomes unstable first. This case corresponds to the lower limit of the estimated stress value τ_{zz}^{min}.

Thus, from the linear analysis, it is already obvious that many scenarios of the instability are possible. Dynamically, many modes can be excited simultaneously while the temperature T increases from T_0 up to the melting point T_{melt}. Even though the first mode becomes unstable first it might happen that further modes play a dominant role creating rather

complex dynamical behaviours. Any particular pattern, of course, depends on temporal characteristics such as the ratio between the instability increment and the temperature rise time.

5. Numerical results

Now, there are two important issues to be investigated. The first is the nature of the instability in the nonlinear stage. The second issue is the magnitude of the longitudinal and transverse stresses in this situation. These issues are investigated by solving nonlinear equation (1) numerically.

5.1. Numerical algorithm

The numerical method of solving equation (1) with the boundary conditions (4) is based on the complete set of orthogonal functions (23).
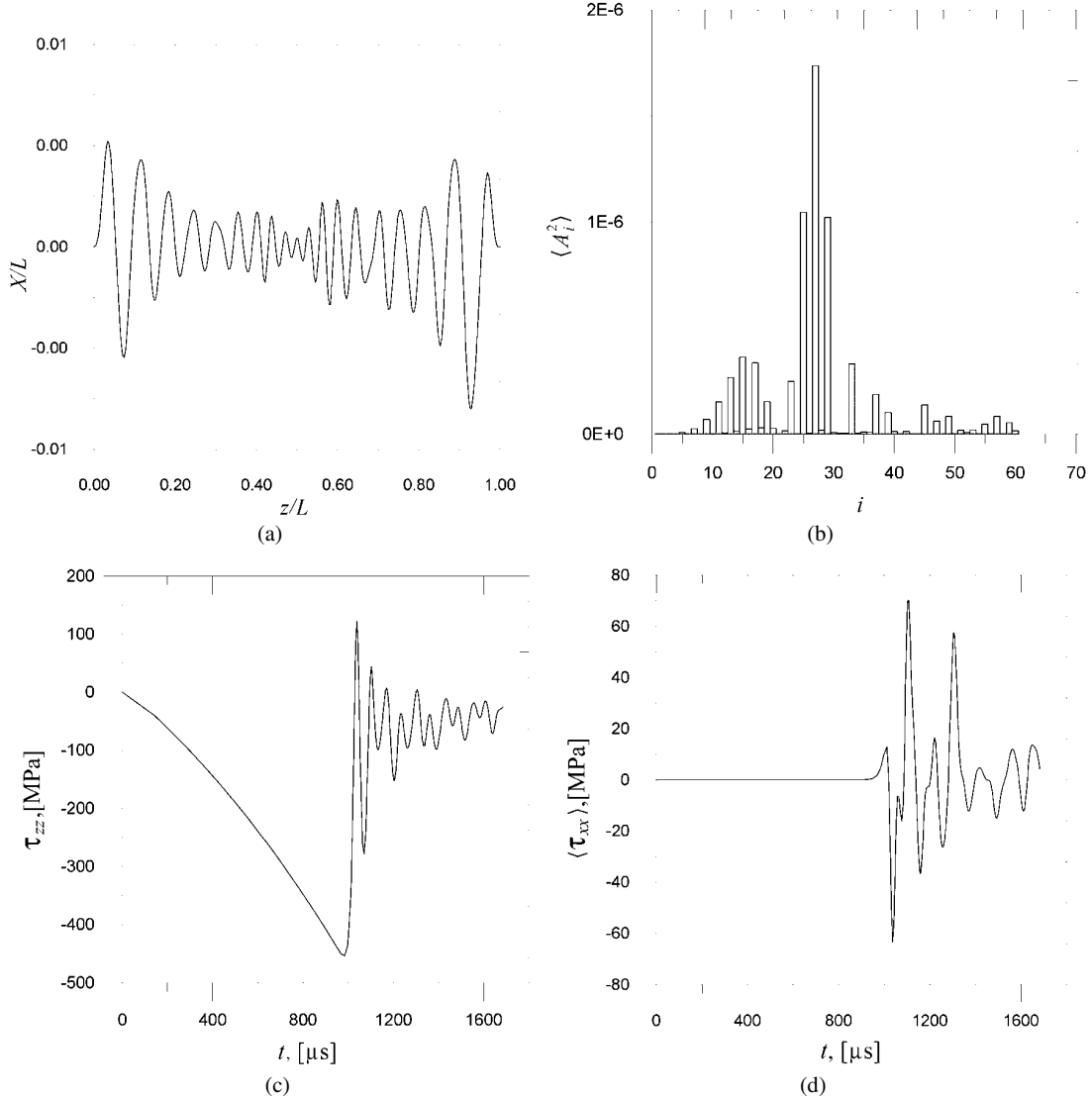
Figure 2. (a) The wire displacement X/L as a function of z/L, case [B]. (b) The spectrum of the wire vibrations at the melting point $\langle A_i^2 \rangle$ as a function of mode number i, case [B]. (c) The longitudinal stress τ_{zz} as a function of time, case [B]. (d) The transverse stress $\langle \tau_{xx} \rangle$ as a function of time at $z/L = 0.9$, case [B].

By expanding any solution to (1) into a series of the functions $\{\mathcal{X}_i\}$, i.e. $X = \sum_i A_i \mathcal{X}_i$, the partial differential equation turns into a system of ODEs with respect to time. They are

$$\sum_j B_{ij} \frac{d^2 A_j}{dt^2} + A_i \frac{\lambda_i^4}{2} + A_i \frac{\lambda_i^2}{2} \{\beta_a(\tilde{l} - \tilde{l}_0 - \alpha[T(t) - T_0])$$

$$+ \beta_B(0.14 + \ln(\lambda_i a/L))\} = 0 \qquad (40)$$

where the coefficients are $\beta_a = 4L^2/a^2$, $\beta_B = (\mu_0 I^2 L^2)/(4\pi EJ)$. The symmetric matrix B_{ij} is given by $B_{ij} = \int_0^1 X_i X_j \, dz$. The length increment is $\tilde{l} - \tilde{l}_0 = \frac{1}{4} \sum_j (A_j^2 - A_j^{0\,2})\lambda_j^2$. The functions X, X_0 and the variable z have been normalized on L, and t has been normalized by $t_0 = \sqrt{(\rho S/EJ)}L^2$. In the numerical simulations, the infinite series have been truncated at the maximal unstable mode defined by (37).

5.2. Flexural vibrations of initially straight wires

In the case of initially straight wires the initial conditions are $A_i(0) = 0$. To excite the instability one needs to set some initial noise level. To simulate noise present an additional fluctuation force in equation (1), $\delta F = \delta F_0 \delta f(t) \sum_i \exp(-\xi_i^2/\xi_1^2)\mathcal{X}_i$, has been added, with the amplitude $\delta F_0 = 4 \times 10^{-4}$ N. The function $\delta f(t)$ is a random number generator producing numbers from the uniform distribution in the interval $[-1, 1]$ at each calculated step over time. The amplitude δF_0 has been chosen to give rise to small deflections $X \sim 0.1a$ of an aluminium wire with $L = 1$ m and $a = 0.6$ mm from a straight line. The form factor $\sum_i \exp(-\xi_i^2/\xi_1^2)\mathcal{X}_i$ has been chosen such that the contribution from the noise source into the first mode X_1 has been dominant, while the other modes are excited as well.

The current profile in the simulations has been taken in the form $I(t) = I_0 \sinh(t/t_0)/\cosh(t/t_0)$, where t_0 is the current rise time. In all runs, $t_0 = 30$ μs. This time is about twice as high as the skin time for aluminium wires with $a = 0.6$ mm,

$t_{skin} = a^2 \sigma \mu_0 \simeq 17 \, \mu$s. The initial temperature has been kept at $T_0 = 300$ K and calculations stopped once the temperature had reached the melting point $T = T_{melt}$. This moment is designated by $t = t_e$.

Simulations have been performed for different conditions: different wire lengths, different currents and different wire materials. All the sets used are presented in table 1.

As the first example, let us consider a short aluminium wire carrying 5 kA current, case [A]. For these parameters from the linear analysis one would expect a few unstable modes to develop, $i_{lim} = 6$. The results obtained are presented in figure 1. In the first two frames, the deflection X as a function of z and the spectrum $\langle A(t)_i^2 \rangle$ both taken at $t = t_e$ have been plotted. In the last two frames, the longitudinal τ_{zz} and transverse $\langle \tau_{xx} \rangle$ stress components have been plotted as functions of time. The spectrum has been calculated by means of averaging over time around $t = t_e$, i.e. $\langle A(t_e)_i^2 \rangle = \int_{t_e - \Delta}^{t_e} A(t)_i^2 \, dt$, where Δ is chosen to be greater than the period of nonlinear vibrations. Both the spectrum (figure 1(b)) and the wire shape, in the form of being close to a simple arc (figure 1(a)), show that the first mode dominates during the nonlinear stage of the instability. Temporal behaviour of the longitudinal and transverse stress components demonstrates developed nonlinear flexural vibrations (figures 1(c) and (d)). The appearance of the instability is clearly seen at $t \simeq 900 \, \mu$s in both figures. The observed longitudinal stress has both compressive and tensile components. The instability appears after strong compression, the maximal compressive stress being 429 MPa. The maximal tensile longitudinal stress amounts to $\tau_{zz} \simeq 244$ MPa. This value is well above the ultimate stress value for aluminium. The observed transverse stress, as has been expected, is lower then the longitudinal value, $\langle \tau_{xx} \rangle \simeq 55$ MPa.

Let us consider now a longer wire, case [B]. This case is relevant to the conditions of Graneau's experiments [4]. One might expect, in accordance with our qualitative analysis, more active modes in the instability spectrum to develop with respect to the previous case, $i_{lim} = 129$. Indeed, from figure 2(a) and (b) one can observe that the spectrum becomes very rich with the major contribution from mode $n = 27$ at the melting point. The tensile longitudinal and transverse stresses amount to $\tau_{zz} = 122$ MPa and $\langle \tau_{xx} \rangle = 92$ MPa in this case; see figures 2(c) and (d). Both stresses are well above the ultimate strength of aluminium. Thus, one might expect the first wire break to appear just after buckling occurs, at $t = 1000 \, \mu$s.

Let us investigate now the effect of variations of current. In case [C], which is a replica of case [B] but with lower current, two modes $n = 5$ and $n = 7$ become dominant (figure 3(a)). This fact indicates, if we compare two spectra in cases [B] and [C], that the main channel of release of the accumulated energy now goes through the modes with lower numbers. Thus, one would anticipate a lower accumulated stress according to our qualitative stress analysis. Indeed, we have observed that both tensile longitudinal and transverse stresses reduce to $\tau_{zz} = 70$ MPa and $\langle \tau_{xx} \rangle = 23$ MPa (figures 3(b) and (c)).

On the other hand, an increase in the current leads to a higher resultant tensile stress value. In case [D], which is similar to set [B] but with a higher current, the longitudinal tensile stress is $\tau_{zz} \simeq 233$ MPa at a maximum
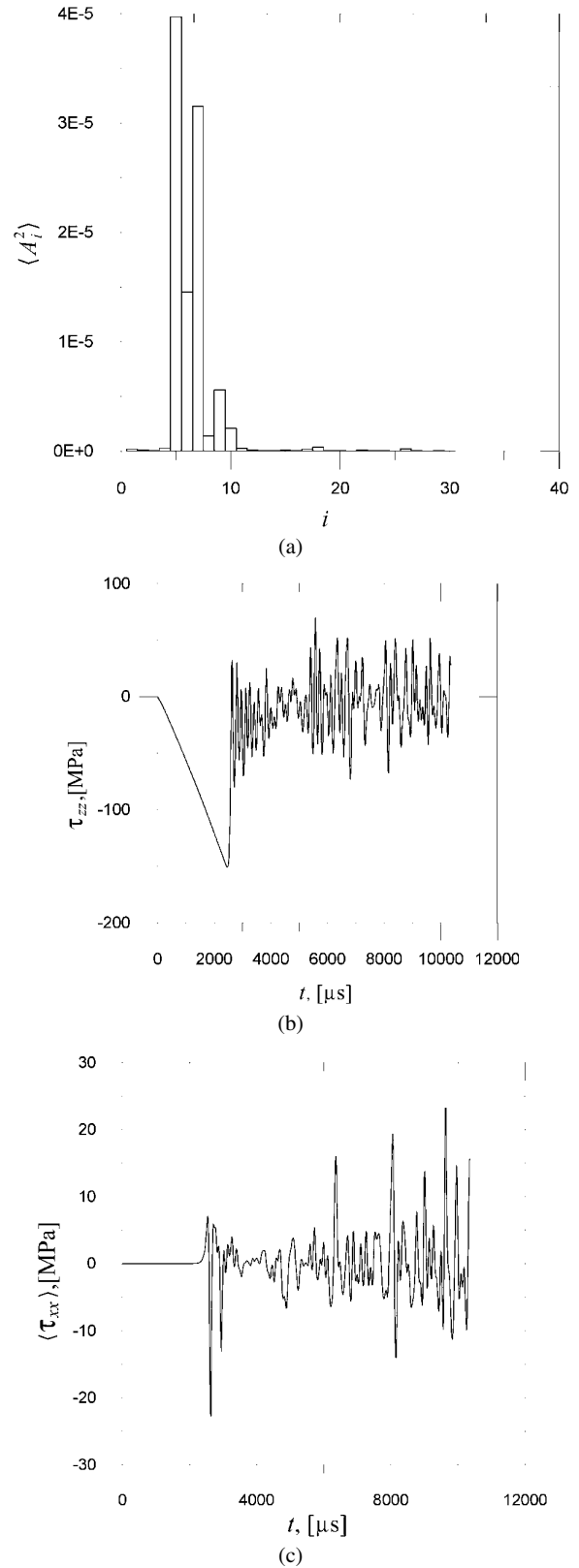

(a)

(b)

(c)

Figure 3. (a) The spectrum of the wire vibrations at the melting point $\langle A_i^2 \rangle$ as a function of mode number i, case [C]. (b) The longitudinal stress τ_{zz} as a function of time, case [C]. (c) The transverse stress $\langle \tau_{xx} \rangle$ as a function of time at $z/L = 0.9$, case [C].

(figure 4). It should be noted that because of faster heating the preliminary compression before the instability develops
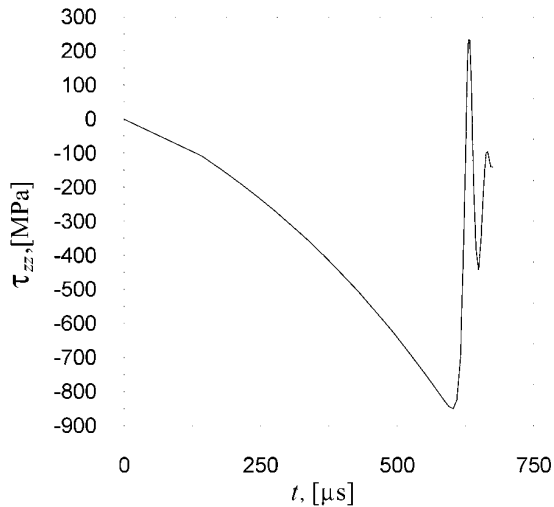
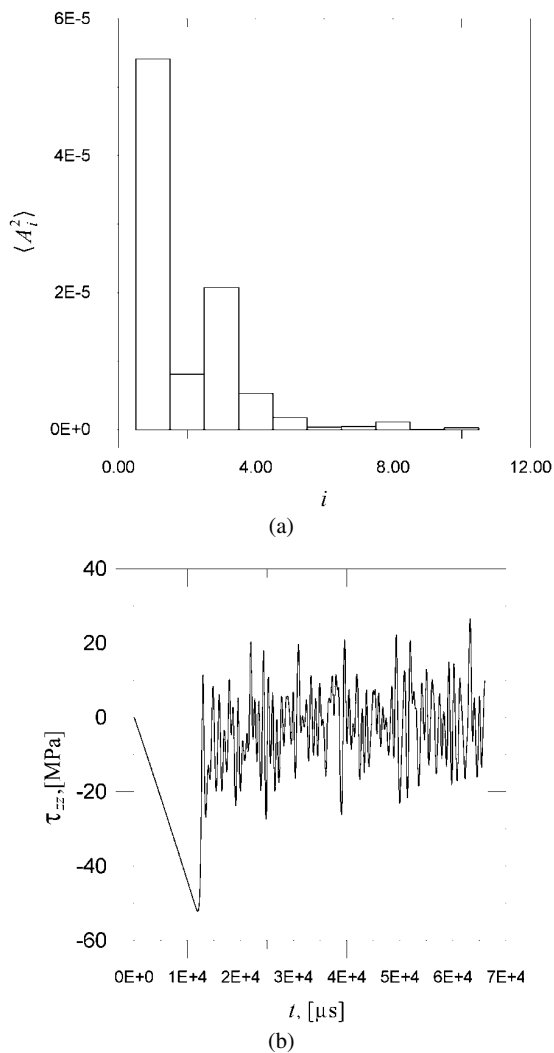**Figure 4.** The longitudinal stress τ_{zz} as a function of time, case [D].

Figure 5. (a) The spectrum of the wire vibrations at the melting point $\langle A_i^2 \rangle$ as a function of mode number i, case [E].
(b) The longitudinal stress τ_{zz} as a function of time, case [E].

is much stronger, namely 851 MPa, and the instability occurs just before the melting point. It appears that at

higher currents the wire will be molten before the buckling occurs.

Let us consider now Nasilovski's experiment with a long copper wire, case [E]. This experiment has been carried out at quite a low current, $I = 500$ A, in comparison with all the previously considered cases. As a result, one might expect low stress values compared to previous cases. Also, the few first modes must be dominant, which is just the case, see figure 5(a). The observed values of stress indeed become quite low. The longitudinal stress reaches $\tau_{zz} \simeq 27$ MPa at a maximum (figure 5(b)), while the transverse stress is just about 4 MPa, which means that the wire can be broken only if it is heated up sufficiently.

5.3. Flexural vibrations of initially bent wires

In the above we considered a somewhat idealized situation, when the undeformed wire had the shape of a straight rod. In reality, the wire might initially have any form. For instance, in the case of horizontal positioning of the wire it might be bent by gravitational force. Once the initial dislocation becomes greater than the radius, the character of the instability changes, as has been discussed. Indeed, if $X_0 \neq 0$ the initial state is unstable from the beginning. However, if the temperature rise time is shorter than the period of flexural vibrations then those modes which contribute into $X_0 = \sum_i A_i^0 \mathcal{X}_i$ can be excited directly. Moreover, buckling on the other modes is still possible. To estimate the stresses developed, simulations for case [B] have been performed but with initial conditions given by $X_0 = A_1^0 \mathcal{X}_1$ with the amplitude taken at $A_1^0 = 20a$. That is, the wire was initially shaped like the first mode of the set (23).

The results of simulations are shown in figure 6. As before, one can see nonlinear vibrations developing. The regular character of the vibrations points out the fact that only one single mode $i = 1$ is active in this case, which means that buckling on the other mode does not occur. The amplitude of tensile longitudinal stress for this particular case amounts to $\tau_{zz} \simeq 50$ MPa. So, a sufficiently heated wire can be broken in this case as well.

6. Conclusions

When an electric current passes through a thin metal wire with clamped ends, flexural elastic stress waves are induced owing to the joule heating and the electromagnetic force. The joule heating leads to thermal expansion of the wire material, which is the dominant mechanism of the excitation of vibrations. Under realistic experimental conditions the electromagnetic force is of minor importance.

Flexural vibrations in an initially straight wire may be excited as a result of the buckling instability. The energy accumulated in the wire during the initial stage in the form of a compressive stress is suddenly released. As a result, high tensile stress appears, which is sufficiently high to cause the fracture of the wire within 1 ms for all the cases considered. The number of modes of the instability that are excited depends on the current magnitude and wire length. Depending on these parameters it is possible to excite just a single mode, which has a form of an arch, or actually any number of modes.
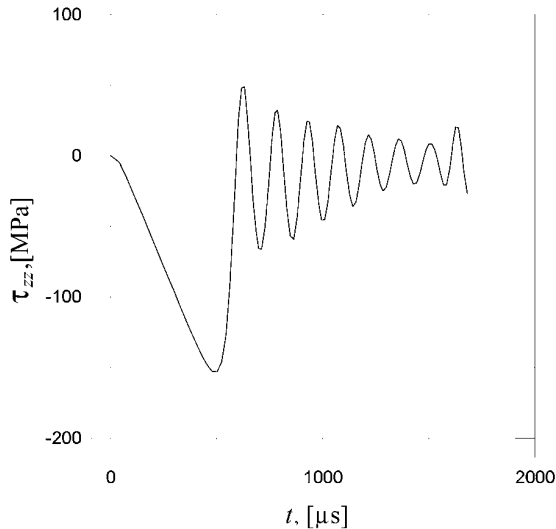
Figure 6. Flexural vibrations of an initially bent wire, longitudinal stress as a function of time; $X_0 = A_1^0 \mathcal{X}_1$, $A_1^0 = 20a$. The wire and current parameters are relevant for case [B].

If a wire is slightly curved, which is a more realistic case than that of the straight wire, the buckling instability is still possible. The amplitude of modes that are initially present in the curved wire grows. The other modes can still be excited in a rapidly heated wire owing to buckling instability. The magnitude of tensile stress induced in a curved wire is clearly lower, but is still sufficient to induce a wire fracture on a millisecond timescale.

Three-dimensional effects, which may be induced by the external circuit, suspensions at the clamped ends, imperfections of the wire cross section or a wire material, will increase the magnitude of tensile stress. These effects will lead to the coupling between flexural, longitudinal, and torsional modes. This study is beyond the scope of the present paper.

The experimental evidence, in general, is supportive of the mechanism described above. However, no direct comparison is possible, since previous experiments were of an exploratory nature.

References

[1] Nasilovski J 1964 Unduloids and striated disintegration of wires *Exploding Eires* vol 3, ed W G Chase and H K Moore (New York: Plenum) p 295
[2] Graneau P 1984 Longitudinal magnet forces? *J. Appl. Phys.* **55** 2598
[3] Graneau P 1984 Ampere tension in electric conductors *IEEE Trans. Magn.* **20** 444
[4] Graneau P 1987 Wire explosions *Phys. Lett.* A **120** 77
[5] Graneau P 1994 *Ampere–Neumann Electrodynamics of Metals* (Palm Harbour, FL: Hadronic)
[6] Hong J S 1994 Electromagnetic forces in flexible systems *DPhil Thesis* University of Oxford
[7] Molokov S and Allen J E 1997 The fragmentation of wires carrying electric current *J. Phys. D: Appl. Phys.* **30** 3131
[8] Ternan J G 1986 Stresses in rapidly heated conductors *Phys. Lett.* A **115** 230
[9] Brandes E A and Brook G B (ed) 1998 *Smithells Metals Reference Book* 7th edn (London: Butterworth)
[10] Landau L D and Lifshitz E M 1970 *Theory of Elasticity* (Oxford: Pergamon) p 89
[11] Thompson W B 1964 *An Introduction to Plasma Physics* (Oxford: Pergamon) p 107
[12] Chattopadhyay S and Moon F 1975 Magnetoelastic buckling and vibration of a rod carrying electric current *J. Appl. Mech.* Dec 809
[13] Landau L D and Lifshitz E M 1984 *Electrodynamics of Continuous Media* (Oxford: Pergamon) p 123
[14] Leontovich M A and Shafranov V D 1961 The stability of a flexiable conductor in a longitudinal magnetic field *Plasma Physics and the Problem of Thermonuclear Fusion Reactions* vol 1 (Oxford: Pergamon)
[15] Chen W F and Atsuta T 1976 *Theory of Beam-Columns* vol 1 (New York: McGraw-Hill)